



## Overview of the deuterium inventory campaign in Tore Supra: Operational conditions and particle balance

B. Pégourié<sup>a,\*</sup>, C. Brosset<sup>a</sup>, E. Tsitrone<sup>a</sup>, A. Beauté<sup>a</sup>, S. Brémond<sup>a</sup>, J. Bucalossi<sup>a</sup>, S. Carpentier<sup>a</sup>, Y. Corre<sup>a</sup>, E. Delchambre<sup>a</sup>, C. Desgranges<sup>a</sup>, P. Devynck<sup>a</sup>, D. Douai<sup>a</sup>, G. Dunand<sup>a</sup>, A. Ekedahl<sup>a</sup>, A. Escarguel<sup>b</sup>, E. Gauthier<sup>a</sup>, J.P. Gunn<sup>a</sup>, P. Hertout<sup>a</sup>, S.-H. Hong<sup>a</sup>, F. Kazarian<sup>a</sup>, M. Kočan<sup>a</sup>, F. Linez<sup>a</sup>, Y. Marandet<sup>b</sup>, A. Martinez<sup>a</sup>, M. Mayer<sup>c</sup>, O. Meyer<sup>a</sup>, P. Monier-Garbet<sup>a</sup>, P. Moreau<sup>a</sup>, P. Oddon<sup>a</sup>, J.-Y. Pascal<sup>a</sup>, F. Rimini<sup>a</sup>, J. Roth<sup>c</sup>, F. Saint-Laurent<sup>a</sup>, F. Samaille<sup>a</sup>, S. Vartanian<sup>a</sup>, C. Arnas<sup>b</sup>, E. Aréou<sup>a</sup>, C. Gil<sup>a</sup>, J. Lasalle<sup>a</sup>, L. Manenc<sup>a</sup>, C. Martin<sup>b</sup>, M. Richou<sup>b</sup>, P. Roubin<sup>b</sup>, R. Sabot<sup>a</sup>

<sup>a</sup> Association Euratom-CEA, CEA/DSM/IRFM, CEA Cadarache, F-13108 Saint-Paul-lès-Durance cedex, France

<sup>b</sup> PIIM, CNRS/Université de Provence, F-13397 Marseille, France

<sup>c</sup> MPI für PlasmaPhysik, Euratom Association, Boltzmannstr. 2, 85748 Garching, Germany

### ARTICLE INFO

PACS:  
52.55.Fa  
52.40.Hf

### ABSTRACT

A specific experiment was performed in Tore Supra, dedicated to the search for consistency between wall inventories estimated from gas balance and post-mortem analysis and to the characterization of the D-retention mechanism. More than 160 similar discharges were performed, representing a cumulative time of 18000 s of plasma with no intermediate conditioning procedure. The only significant operational issue was linked to the ejection of flakes from the plasma facing components, whose frequency increased dramatically during the campaign, triggering a plasma detachment phase followed by a disruption in number of cases. In-vessel inventory was increased by  $\sim 3.1 \times 10^{24}$  D, and constant retention rate ( $\sim 2.3 \times 10^{20}$  D/s averaged over discharge duration) was measured, with no indication of wall saturation. First measurements on dismantled tiles of the Toroidal Pump Limiter (TPL) show [D]/[C] ratios ranging from 0.04 to 0.20, on a typical thickness of 15–20  $\mu\text{m}$ . Extrapolated to the whole TPL, this yields an amount of  $\sim (1.5 \pm 0.3) \times 10^{24}$  D, i.e.  $\sim 50\%$  of the estimated in-vessel inventory.

© 2009 Elsevier B.V. All rights reserved.

### 1. Introduction

In-vessel tritium retention is a crucial issue for ITER and numerous experiments were devoted to its characterization, in metal as well as carbon wall machines [1]. Considering the initial design of the ITER wall (i.e. with a carbon divertor), a simple extrapolation of present measurements shows that the limit of 700 g set by nuclear licensing could be reached in few 100 $\times$  nominal discharges. However, although the general trend is well established and observed in many devices, the underlying physical process is not clearly identified and retention rates deduced from integrated particle balance ( $\sim 10$ – $20\%$  of the injected gas,  $>30\%$  in Tore Supra) are significantly larger than those estimated from post-mortem analysis of the Plasma Facing Components (PFCs;  $\sim 3$ – $4\%$ ) [2]. Comparing these two estimates is difficult, since the former is generally

based on particle balance calculations for a limited number of discharges when the latter integrates the whole history of PFCs. To clarify the discrepancy between these two methods for determining the fuel retention, the only way is thus to load the wall with deuterium in a controlled discharge scenario until its inventory is known with high enough accuracy from integrated particle balance, and then to dismantle the PFCs for analysis. Such a study was undertaken in Tore Supra, composed of three phases: a dedicated campaign to load the PFCs with deuterium, the dismantling of a limiter sector to extract selected samples, then an extensive analysis program on the samples. This paper presents an overview of the wall loading experiment and results on the D-content of 10 dismantled tiles of the Toroidal Pumped Limiter (TPL). It presents first the time schedule of the campaign and main operational issues, then the characteristics of plasma-wall interaction, erosion and retention rates as well as the integrated amounts of eroded carbon and trapped deuterium, and finally the first measurements of the D-content for few selected samples. Main results and implication for next step devices are summarized in the last section.

\* Corresponding author.

E-mail address: [bernard.pegourie@cea.fr](mailto:bernard.pegourie@cea.fr) (B. Pégourié).

## 2. Operation

### 2.1. Schedule of the experimental campaign

A  $^{13}\text{C}$  carbonization and a boronization were performed prior to the beginning of the experiment itself (equivalent deposition of  $\sim 2 \times 80$  monolayers of  $\text{a-}^{13}\text{C:H}$  and  $\text{a-B:D}$  for a uniform coating of the vessel) for marking the beginning of the experiment by a  $^{13}\text{C}$ -layer easily identifiable in subsequent analysis and for minimizing oxygen and metals before long cumulative time of operation without other conditioning procedure. The goal was to increase in a controlled way the in-vessel D-inventory by a significant factor (from 4 to 5) with respect to its pre-campaign value, estimated to be  $W_{\text{init}} \sim 8 \times 10^{23} \text{ D}$  [3], but known with a insufficient accuracy to be reasonably compared with post-mortem analysis. A robust scenario was designed, allowing plasma duration long enough ( $\sim 125 \text{ s}$ , with flat top  $> 115 \text{ s}$ ) for permanent retention to be much larger than post-discharge recovery, namely: average density  $\langle n_e \rangle = 1.5 \times 10^{19} \text{ m}^{-3}$ , Lower Hybrid (LH) power  $P_{\text{LH}} = 2 \text{ MW}$ , plasma current  $I_p = 0.6 \text{ MA}$  and magnetic field  $B_T = 3.8 \text{ T}$ . Active pumping was provided by the TPL (10 torbomolecular pumps of pumping speed  $S = 2 \text{ m}^3/\text{s}$  each) and the average time between two successive discharges was  $\sim 20 \text{ min}$ .

Ten days, distributed over 3 weeks, were devoted to the D-loading of the wall. Main operational issue was linked to the ejection of flakes, whose frequency increased dramatically during the campaign, the largest triggering a phase of plasma detachment followed by a disruption in a number of cases. This is shown in Fig. 1, where the number of events per discharge (the selection criterion is an increase  $> 20\%$  of the radiated power  $P_{\text{rad}}$ ) is plotted vs. discharge number, showing an almost linear increase and a correlated decrease of the plasma duration due to the increasing frequency of disruptions. After  $\sim 220$  discharges, operation was so difficult and disruptions so frequent (see Fig. 1(c)) that it became necessary to modify the LH-power waveform, from a constant value to a continuous ramp up starting from  $1.2 \text{ MW}$  and reaching  $1.6\text{--}1.8 \text{ MW}$ . The consequence of this limitation of  $P_{\text{LH}}$  was a decrease of the plasma duration down to  $\sim 90 \text{ s}$ . The right part of Fig. 1 shows that, after some discharges devoted to scenario optimization, this modification allowed to operate with almost no disruptions even if an increase of the frequency of flake ejections was

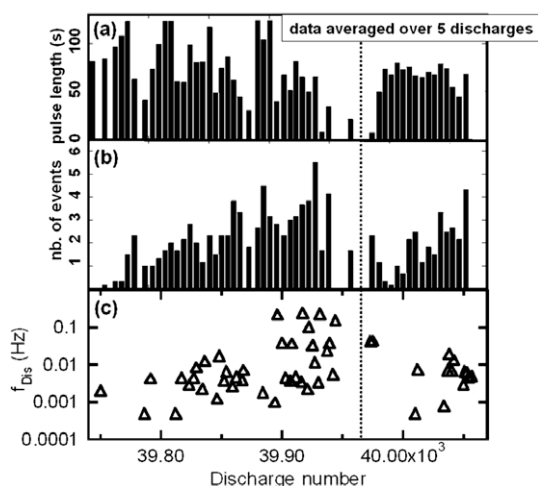


**Fig. 1.** (a) Pulse duration; (b) number of flake ejections per discharge vs. discharge number. Data are averaged over five discharges; and (c) frequency of disruptions (with respect to plasma duration). The vertical line indicates the change in plasma scenario.

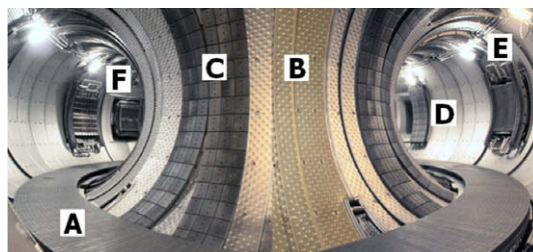


**Fig. 2.** Tore Supra in the CIEL configuration: (A) TPL, (B) stainless steel panels, (C) poloidal bumpers, (D) OML, (E) IC-antenna, and (F) LH-launchers.

yet observed. At the very end of the campaign, attempts were made to search for the  $P_{\text{LH}}$  limit, showing that – for such wall conditions – it is close to  $\sim 1.9 \text{ MW}$ .

### 2.2. Disruption analysis

A photograph of Tore Supra in the CIEL (Composants Internes Et Limiter) configuration is displayed in Fig. 2 (see [4] for a detailed description). The major component is the TPL, which consists of a flat toroidally continuous ring made of 12000 Carbon Fiber Composite (CFC) tiles. A set of 12 poloidal bumpers on the high field side and an Outboard Movable Limiter (OML) on the low field side, all armored with brazed CFC tiles, protect the inner wall and the RF-antennae from transient events such as disruptions. The total surface of the vacuum vessel covered with carbon CFC tiles is  $\sim 15 \text{ m}^2$ ; whose  $\sim 3.5 \text{ m}^2$  in close interaction with the plasma. All the PFCs are actively cooled with a pressurized water loop allowing them to reach thermal equilibrium in less than 1s for the TPL, up to  $\sim 10 \text{ s}$  for the bumpers. In this configuration, the typical temperature increase of the TPL surface is  $\sim 200 \text{ }^\circ\text{C}$  for 3 MW of additional power. So far,  $450 \text{ }^\circ\text{C}$  is the highest temperature measured on clean tile surface in the regions of strong interaction with the plasma. However, deposits reach much higher temperatures, from  $\sim 500$  to  $600 \text{ }^\circ\text{C}$  at medium power to up to  $> 1500 \text{ }^\circ\text{C}$  at high power for the thickest.

The surface Infra-Red (IR) emission of the LH launchers and of  $\sim 1/4$  of the TPL is monitored by IR-cameras for following the PFCs temperature (or that of the deposits at their surface). It allows also the visualization of flake ejection. Among the 62 disruptions encountered during the experiment,  $\sim 85\%$  are monitored by the IR-cameras [5]. In most cases, a localized hot spot appears in a thick deposit region,<sup>1</sup> yielding moderate density increase due to local outgassing. A MARFE is triggered, the radiated power increases (dominated by carbon radiation) and a flake is ejected. In case of major perturbations, the LH-power is switched-off by the security system in response to the edge perturbation, yielding a disruption.

Even more than the absolute number of flake ejections per discharge (among the  $\sim 500$  events detected – see Fig. 1, only  $\sim 12\%$  led to a disruption), the most remarkable characteristic of this experiment is the continuous increase of their occurrence. Two specific circumstances can possibly explain this behaviour: (1) the long plasma time without conditioning and (2) the systematic repetition of the same plasma scenario. The first one is unlikely, since no increase of the flake ejection frequency was observed in previous campaigns with time delay between two conditioning procedures (He-glow cleaning, boronizations). Conversely, the second can favour the build up of thick deposits in the shadowed regions of the TPL surface – in the immediate vicinity of the confined plasma – since the footprint of the plasma on the TPL remained un-

<sup>1</sup> A picture of the deposit pattern at the surface of the TPL can be seen in Fig. 4 (centre).

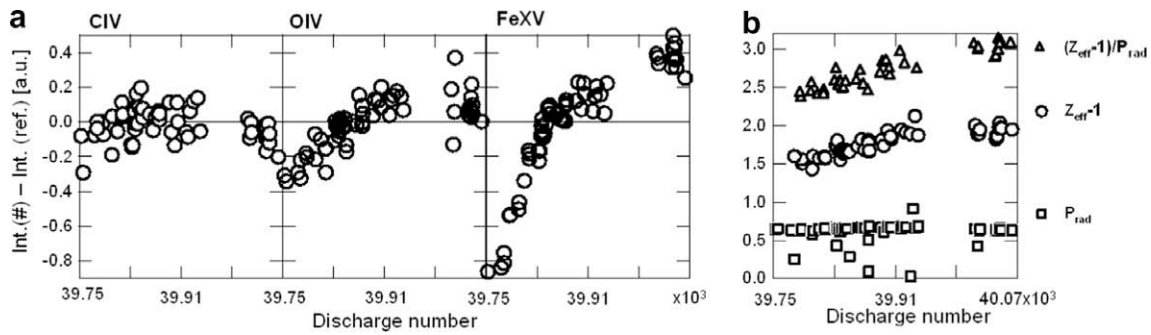


**Fig. 3.** (a) Variation of intrinsic impurity radiance vs. discharge number. The variations are relative to the radiance level in the reference pulses before carbonization and boronization (zero line). The error on the measurements, mainly from statistical variations, is estimated to be  $\pm 20\%$ . (b) Effective charge ( $Z_{\text{eff}} - 1$ ), total radiated power ( $P_{\text{rad}}$ ) and ratio  $(Z_{\text{eff}} - 1)/P_{\text{rad}}$  vs. discharge number.



**Fig. 4.** CII and CD emission lines intensity distribution at the TPL surface. The central picture shows the field of view of the endoscope and the different zones discussed in this paper: erosion (shiny), thin deposits (bluish/black) and thick deposits (grey/looking coarse).

changed during the whole experiment ( $\sim 5$  h of continuous discharge).

### 3. Particle balance from gas balance

#### 3.1. Plasma behaviour

Although no conditioning procedure was performed during the whole experiment, the main plasma parameters remained remarkably constant: no uncontrolled increase of the density was observed, neither any change in the density ( $n_{e0} = 2.7 \times 10^{19} \text{ m}^{-3}$ ) and temperature profiles ( $T_{e0} \sim 3.5 \text{ keV}$ ), nor in the edge characteristics ( $n_{e\text{LCFS}} = 2 \times 10^{19} \text{ m}^{-3}$ , e-folding length  $\lambda_n = 7 \text{ cm}$ ,  $T_{e\text{LCFS}} = 25 \text{ eV}$ ,  $\lambda_T = 6 \text{ cm}$ ,  $T_{i\text{LCFS}} \sim 3.5 \times T_{e\text{LCFS}}$ ). The time history of plasma radiation and impurity content is displayed in Fig. 3. If the intensity the C-IV ( $\lambda = 28.92 \text{ nm}$ ) emission line remains constant, that of the Fe-XV ( $\lambda = 28.42 \text{ nm}$ ) and O-IV ( $\lambda = 27.20 \text{ nm}$ ) lines are initially very low due to the carbo-boronization that marks the beginning of the experiment, but they recover their pre-campaign value after  $\sim 3000$  s of plasma and then continue to increase moderately by  $\sim 25\%$  up to the end of the experiment [6]. The absence of variation of the radiated power shows that it is always dominated by carbon radiation, even if the moderate increase of Z-effective and of the brightness of the peripheral emission lines of O and Fe demonstrates a moderate increase of the impurity content.

#### 3.2. Plasma surface interaction

The TPL surface is observed in  $D\alpha$  ( $D\gamma$ ), CII and CD light by two cameras equipped with multiple filters and four optical fibres coupled to a Czerny-Turner spectrometer [7]. Typical light distribution in the CII ( $\lambda = 515 \text{ nm}$ ) and CD ( $\lambda = 431 \text{ nm}$ ) lines are displayed in Fig. 4. In both cases, the zones in direct interaction with the plasma (erosion zones) are clearly visible, but specific features differ depending on the observed wavelength. In the CII line, they are

the deposits in the inter-tile gaps close to the tangency point of the Last Closed Flux Surface (LCFS) on the TPL when, in the CD band, it is the leading edge of the TPL. In addition, transient CD spots were observed close to the LCFS tangency point, but without clear correlation with an increase of the temperature surface or with a flake ejection.

The total erosion rate,  $Y_{\text{tot}}$ , is estimated from the CII/ $D\alpha$  flux ratio to be  $\sim 1\%$  in the erosion zone, and  $\sim 0.7\%$  on the deposits, with no significant change during the campaign. In what concerns the chemical erosion rate, the low S/N ratio of the CD measurements does not allow an accurate estimate, and only an upper limit  $Y_{\text{chem}} < 1\%$  can be deduced from collected data. These values are in close agreement with those deduced from the global (experimental and modelling) study of carbon migration in Tore Supra described in [8]. Thus, the scaling law for total carbon production deduced from this work ( $dN_C/dt = 5 \times 10^{20} \times (P_{\text{tot}} - P_{\text{rad}}) \text{ C/s}$ ) can be used to estimate the total gross erosion during the present campaign, yielding a total of  $N_C \sim 1.15 \times 10^{25}$  eroded C atoms ( $\sim 230 \text{ g}$ ).

#### 3.3. Increment of wall D-inventory

Particle balance measurements were done for every discharge. The different terms involved are displayed in Fig. 5, which shows – as a function of the discharge number – the amount of gas injected ( $Q_{\text{inj}}$ ), pumped ( $Q_{\text{exh}}$ ) or outgassed after the plasma termination ( $Q_{\text{post}}$ ),<sup>2</sup> and – as a function of the discharge duration – the increment of the wall D-inventory  $\delta_{\text{WI}} = Q_{\text{inj}} - (Q_{\text{exh}} + Q_{\text{post}})$ . The maximum values for  $Q_{\text{inj}}$  and  $Q_{\text{exh}}$ , which correspond to discharges of nominal duration, remain remarkably constant for a given scenario, emphasizing that the wall recycling properties did not evolve during the experiment. The values of  $Q_{\text{post}}$  are by far less

<sup>2</sup>  $Q_{\text{exh}}$  and  $Q_{\text{post}}$  are corrected from the weak proportion of  $\text{CD}_4$  ( $\sim 2\%$ ) present in the pumped gas.

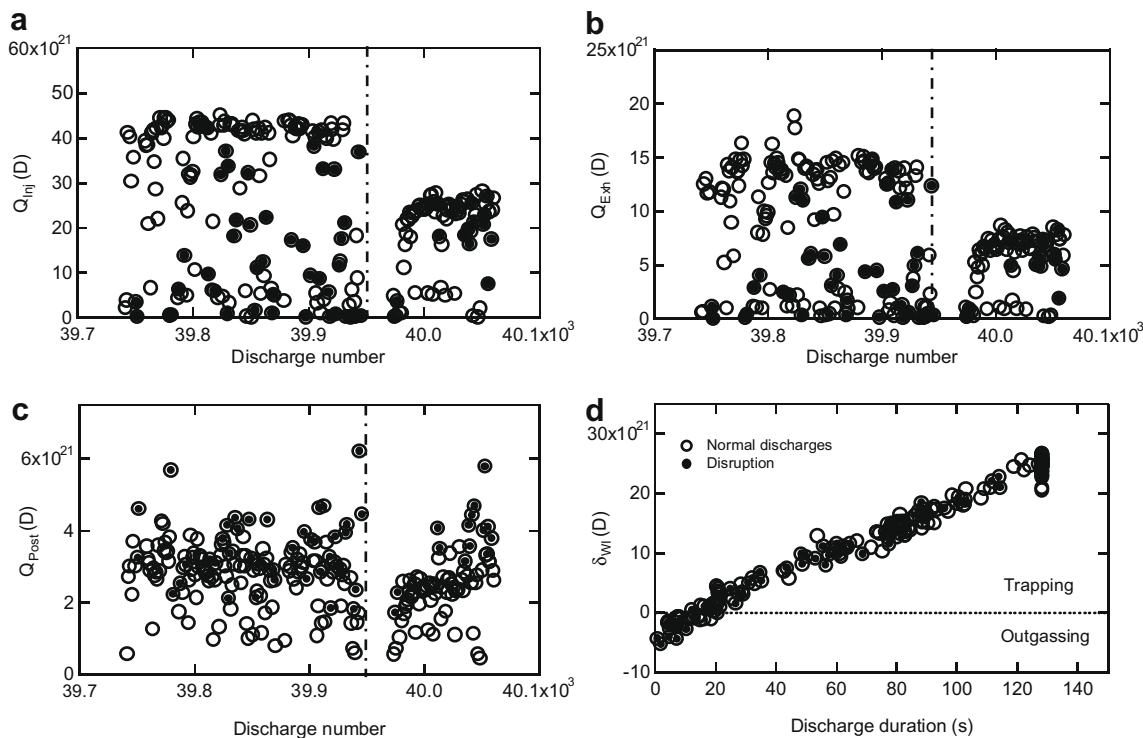


**Fig. 5.** (a) Injected gas per discharge  $Q_{inj}$ , (b) exhausted gas  $Q_{Ext}$ , (c) post-discharge outgassing  $Q_{Post}$  vs. discharge number (the vertical dashed line marks the change in the plasma scenario) and (d) increment of wall D-inventory  $\delta_{WI}$  vs. discharge duration.

sensitive to discharge duration and their value for disruptive discharges is only  $\sim 25\%$  higher than the average  $\langle Q_{Post} \rangle \sim 3 \times 10^{21}$  D, demonstrating that disruptions have only a minor weight in the overall balance. As a result,  $\delta_{WI}$  increases linearly with plasma duration (Fig. 5(d)), demonstrating a constant D-retention (transient + permanent) of  $\sim 2.3 \times 10^{20}$  D/s. Taking into account the post-discharge outgassing, the built up of the wall D-inventory during the whole campaign reaches  $\sim 3.3 \times 10^{24}$  D. This value must be corrected from the  $[H]/[D]$  ratio of the pumped gas due to the hydrogen trapped in the vessel during the initial  $^{13}\text{CH}_4$  carbonization ( $\sim 18\%$  at the beginning, falling down to  $\sim 2\%$  after  $\sim 3000$  s of plasma) and from the amount of D pumped during nights and week-ends ( $\sim 2 \times 10^{23}$  D). As a result, the total in-vessel D-inventory, just before the dismantling of the TPL sector, is estimated to be  $WI_{GB} \sim 3.1 \times 10^{24}$  D.<sup>3</sup>

#### 4. Particle balance from post-mortem analysis

##### 4.1. D-content measurements

Consecutively to the dismantling of a sector of the TPL (20° toroidal), 40 CFC tiles (over a total number of 672) – distributed over erosion, thin and thick deposits zones – were extracted and sampled for analysis. Each tile was cut in three layers (2 mm each) in its thickness. Thermodesorption (TDS) and Nuclear Reaction Analysis (NRA) measurements were performed for a first set of 10 tiles (5, 2 and 3 from erosion, thin and thick deposits zones). Only top – in direct interaction with the plasma – and medium samples were analyzed. No investigation was performed on those located at the bottom of the tiles – at the junction with the Cu/

Cr/Zr heat sink – because of the presence of significant copper infiltration due to the manufacturing process (active metal casting).

TDS measurements were performed up to a maximum temperature of 1200 °C (heating rate 60 °C/min) for the top samples, and 900 °C for the medium samples, due to the presence of remaining copper infiltrations. Due to the way the samples are cut off, TDS measurements take also into account the deuterium trapped in the deposits located on the lateral faces. The measured D-contents of the top samples are displayed in Table 1, where error bars characterize the dispersion of the measurements. The D-content of medium samples (corrected from temperature limitation) is low,  $\sim 5\%$  of that of top samples.

The D content was also measured with NRA using a  $^3\text{He}$  beam (current from 1 to 10  $\mu\text{A}$ , spot size  $\sim 1 \text{ mm}^2$ ) at four energies (0.8, 2.5, 4 and 6 MeV) to produce  $\text{D}(^3\text{He,p})^4\text{He}$  reactions. Quantitative results and deuterium depth profiles were obtained using the simulation program SIMNRA [9]. The averaged  $[D]/[C]$ -profiles over the first 35–40  $\mu\text{m}$  of the top samples (tile surface) are plotted for each zone in Fig. 6. They show significant dispersion (from 30% to 50%, error bars on Fig. 6); not only from sample to sample, but also as a function of the zone analyzed in a given sample. D-concentration is maximum close to the surface and ranges from  $\sim 0.05$  (erosion zone) to  $\sim 0.2$  (deposits), with a typical depth from  $\sim 15$  to 25  $\mu\text{m}$  (erosion zone and thin deposits) to that of the whole layer probed by the beam (thick deposits, mainly due to 1 sample). The D-concentration in the medium samples is always very low (from 0.1% of that of the top samples in the deposits to 2–6% in the eroded regions), even not measurable in a number of cases. Nevertheless, this indicates a deep penetration of the deuterium in the CFC. Except for thin deposits, D-contents determined from NRA are smaller than those measured by TDS. This is mainly due to the fact that the deuterium trapped in the deposits on the lateral faces of the samples is detected by TDS but not by NRA, although one cannot exclude the presence of deuterium deep into the samples, at a distance larger than that probed by the  $^3\text{He}$  beam. Last,

<sup>3</sup> Due to the large uncertainty attached to the value of  $WI_{init}$ , its contribution was not considered in the evaluation of  $WI_{GB}$ .



**Table 1**

Deuterium content per unit area (Top) and extrapolated TPL D-inventory (Bottom) for Erosion, thin deposits and thick deposits zones. For each zone, the combination of NRA and TDS measurements allows to give the D-contents of the surface facing the plasma (tile) and of the lateral faces (in gaps) of the samples.

	TDS (tile + in gaps)	NRA (tile surface)	NRA (in gaps)
<i>D-content (atoms/m<sup>2</sup>)</i>			
Erosion	$(1.1 \pm 0.2) \times 10^{23}$	$(3.6 \pm 1.3) \times 10^{22}$	$(1.4 \pm 0.5) \times 10^{23}$
Thin deposits	$(1.5 \pm 0.3) \times 10^{23}$	$(1.9 \pm 0.3) \times 10^{23}$	$(3.3 \pm 0.6) \times 10^{21}$
Thick deposits	$(6.2 \pm 0.5) \times 10^{23}$	$(3.6 \pm 2.9) \times 10^{23}$	$(1.1 \pm 0.3) \times 10^{23}$
	Tile surface	In gaps	Total
<i>TPL extrapolated D-inventory (atoms)</i>			
Erosion	$1.6 \times 10^{23}$	$4.9 \times 10^{23}$	$6.5 \times 10^{23}$
Thin deposits	$4.8 \times 10^{23}$	$1.0 \times 10^{22}$	$4.9 \times 10^{23}$
Thick deposits	$2.8 \times 10^{23}$	$5.3 \times 10^{22}$	$3.4 \times 10^{23}$

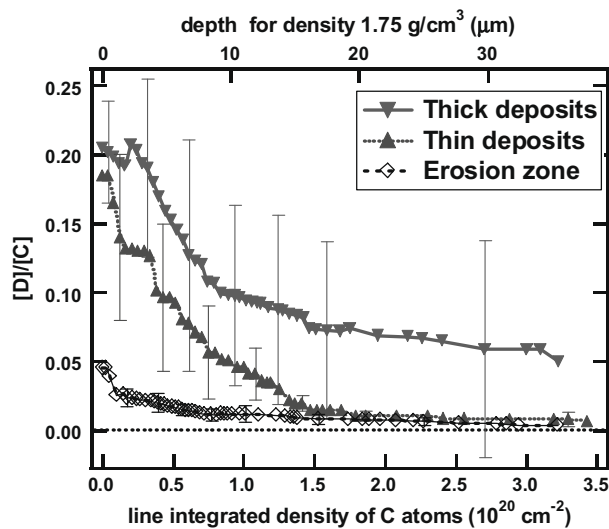


**Fig. 6.** Average  $[D]/[C]$  ratio deduced from NRA measurements vs. line integrated density of C atoms (bottom axis) and depth (assuming a carbon density of  $1.75 \text{ g/cm}^3$ , top axis) for Thick deposits, Thin deposits and Erosion zones. Vertical bars show the dispersion from sample to sample. The surface roughness is  $\sim 5 \mu\text{m}$ .

NRA measurements were also performed on the lateral faces of the tiles, only showing a significant D-content in the erosion and thick deposits region. The values resulting from these measurements are displayed in Table 1.

#### 4.2. Comparison with gas-balance inventory

The D-contents mentioned above can be used for a first estimation of the TPL-inventory. Considering  $3.5 \text{ m}^2$  of eroded zone,  $3 \text{ m}^2$  of thin deposits and  $0.5 \text{ m}^2$  of thick deposits, one obtains  $WI = (1.5 \pm 0.2) \times 10^{24} \text{ D}$ . This number represents  $\sim 50\%$ <sup>4</sup> of the increment of the in-vessel inventory, estimated in Section 3.3 to be  $WI_{CB} = 3.1 \times 10^{24} \text{ D}$ . However, one must keep in mind that this estimation is a lower limit of the whole in-vessel inventory, since no information is yet available on the inner bumpers, whose total surface is  $7 \text{ m}^2$ , also partly covered of potentially D-rich layers.

The deposits present on the other PFCs (neutralizer fingers, RF-launchers and OML) were analyzed in a previous study, showing only a low D-content ( $\sim 10^{23} \text{ D}$ ,  $\sim 10\%$  of the pre-campaign gas-balance inventory) [10]. This difference in the D-content of the different deposits can be understood when considering that those of Ref. [10] were scrapped far from the LCFS, but at places where they are

exposed to significant plasma flux, whereas those on the TPL surface are located in private flux regions, where heating is due to radiation and CX atoms, with almost no plasma flux even if geometrically closer to the LCFS [8].

#### 4.3. Retention mechanism

Despite the small number of measurements available, it can be firmly concluded that the D-retention is dominated by the deposits, since  $\sim 90\%$  of the deuterium already found is located in the coated zones of the TPL and since other PFCs, which are only intermittently or exceptionally in interaction with the plasma, are subject to deposition rather than erosion.

It remains that the amount of deuterium found in the eroded zones of the TPL is much larger and much more deeply implanted than what can be expected from simple stopping length calculations. This can be possibly understood by considering the porosity of the N11 CFC-material, which displays a variety of pores from few nm to few  $10 \times \mu\text{m}$  thickness, yielding a specific area (BET area) of  $\sim 0.3 \text{ m}^2/\text{g}$  and a proportion of vacuum of  $\sim 0.2$  with respect to perfect graphite. For  $1 \text{ m}^2$  of TPL surface over  $15 \mu\text{m}$  depth (average thickness of D-concentration in the erosion zones), this corresponds to  $\sim 9 \text{ m}^2$  of specific area and  $3 \text{ cm}^3$  of voids. If the reservoir associated to a simple coating of the pore surface by D atoms ( $\leq 10^{19} \text{ D/m}^2$ ) is negligible ( $\sim 10^{20} \text{ D}$ ), that due to the filling up of pores consecutively to hydrocarbon deposition is considerable [11]. Assuming a  $[D]/[C]$  ratio  $\sim 0.4$  and a density of  $\sim 1 \text{ g/cm}^3$  for the carbon layers, one finds  $\sim 6 \times 10^{22} \text{ D/m}^2$ , i.e.  $\sim 2 \times$  the D-content per unit of area measured in the erosion zones ( $\sim 3.6 \times 10^{22} \text{ D/m}^2$ ). Even if the part relative to close porosity is not taken into account in the present estimation, the available reservoir is large enough for one to speculate that this process is effectively at work and explains at least partly the D-retention in eroded zones.

#### 5. Summary

An accurate knowledge of the in-vessel D-inventory is essential for a pertinent comparison of gas balance measurements and post-mortem analysis of Plasma Facing Components. For this reason, 10 days were devoted to loading with deuterium the wall of Tore Supra. More than 160 long ( $>1 \text{ min}$ ), identical discharges were performed, for a total time of  $\sim 5 \text{ h}$  of plasma. Despite the fact that no wall conditioning was performed, the macroscopic plasma parameters (density, temperature, radiated power) remained remarkably constant. Main operational issue was linked to flake ejections, whose frequency increased dramatically during the campaign, the largest triggering plasma detachments and numerous disruptions. A constant retention rate was measured ( $\sim 2.3 \times 10^{20} \text{ D/s}$  averaged over the plasma duration), with no sign of wall saturation, leading to a total increment of the wall inventory of  $\sim 3.1 \times 10^{24} \text{ D}$  ( $\sim 4 \times$  pre-campaign estimation). First measurements of the D-content of 10 tiles extracted from the Toroidal Pumped Limiter showed surface D-concentration of  $\sim 5\%$  and  $\sim 20\%$  in the eroded and deposited zones, on typical thickness of  $15\text{--}20 \mu\text{m}$ . Extrapolated over the whole Toroidal Pumped Limiter, this corresponds to  $\sim 50\%$  of the total inventory, widely dominated by the coated zones. Nevertheless, a relatively large amount of deuterium was found deep in the erosion zones, likely due to the high porosity of the CFC material.

In addition to these results, it was observed that the continuous repetition of identical discharges is likely to amplify the characteristics of the C-deposition pattern, because there is no smearing or erosion of deposits due to changes in the plasma geometry. This factor is believed to be responsible for a large part for the increasing number of flake ejections detected during the D-loading campaign. However, although such behaviour can be a critical

<sup>4</sup> No account was taken here of a possible loss of deuterium or isotopic exchange during the period between the time of the TPL-sector dismantling and that of the D-content analysis ( $\sim 6$  months).

issue in any operational schedule, it must be underlined that the specificity of limiter devices probably amplifies the reaction of the plasma to the flake ejections. The main reason is that – in a limiter configuration – the private flux regions in which the deposits grow are very close to the Last Closed Flux Surface. It follows from such geometrical arrangement that any ejected flake has a significant probability to penetrate and perturb the confined plasma, in any case much larger than in a divertor configuration.

## References

- [1] T. Loarer, Fuel Retention in Tokamaks, *J. Nucl. Mater.* 390–391 (2009) 20.
- [2] T. Loarer et al., *Nucl. Fus.* 47 (2007) 1112.
- [3] E. Tsitrone et al., IAEA-CN-116 (Proc. 20th Int. Conf. Vilamoura, 2004), IAEA, EX/10-2, 2004.
- [4] J. Jacquinet, IAEA-CN-94 (Proc. 19th Int. Conf. Lyon, 2002), IAEA, OV/1-2, 2003.
- [5] A. Ekedahl et al., Using IR-Imaging, *J. Nucl. Mater.* 390–391 (2009) 806.
- [6] O. Meyer et al., Impurity Production Monitoring During RF-Experiments on Tore Supra, *J. Nucl. Mater.* 390–391 (2009) 1013.
- [7] E. Delchambre et al., Characterization of Carbon Erosion on the Limiter of Tore Supra, *J. Nucl. Mater.* 390–391 (2009) 65.
- [8] J.T. Hogan et al., IAEA-CN-149 (Proc. 21th Int. Conf. Chengdu, 2006), IAEA, EX/P4-8, 2007.
- [9] M. Mayer, SIMNRA User's Guide, Technical Report IPP 9/113, Max-Planck-Institut für Plasmaphysik, Garching, 1997.
- [10] C. Brosset et al., *J. Nucl. Mater.* 337–339 (2005) 664.
- [11] H. Khodja et al., *Nucl. Instr. and Meth. in Phys. Res. B* 266 (2008) 1425.